Effects of mtDNA in SHR-mt^{F344} versus SHR conplastic strains on reduced OXPHOS enzyme levels, insulin resistance, cardiac hypertrophy, and systolic dysfunction

Josef Houstek, Marek Vrbacký, Katerina Hejzlarová, Václav Zídek, Vladimír Landa, Jan Silhavý, Miroslava Simáková, Petr Mlejnek, Ludmila Kazdová, Ivan Miksík, Jan Neckár, Frantisek Papousek, Frantisek Kolár, Theodore W. Kurtz and Michal Pravenec

Physiol. Genomics 46:671-678, 2014. First published 29 July 2014;
doi:10.1152/physiolgenomics.00069.2014

Physiological Genomics publishes results of a wide variety of studies from human and from informative model systems with techniques linking genes and pathways to physiology, from prokaryotes to eukaryotes. It is published quarterly in January, April, July, and October by the American Physiological Society, 9650 Rockville Pike, Bethesda MD 20814-3991. ISSN: 1094-8341, ESSN: 1531-2267. Visit our website at http://www.the-aps.org/.

Physiol Genomics 46: 671–678, 2014.
First published July 29, 2014; doi:10.1152/physiolgenomics.00069.2014.

CALL FOR PAPERS | *Mitochondrial Metabolism*

Effects of mtDNA in SHR-mt^{F344} versus SHR conplastic strains on reduced OXPHOS enzyme levels, insulin resistance, cardiac hypertrophy, and systolic dysfunction

Josef Houštěk,[1] Marek Vrbacký,[1] Kateřina Hejzlarová,[1] Václav Zídek,[1] Vladimír Landa,[1] Jan Šilhavý,[1] Miroslava Šimáková,[1] Petr Mlejnek,[1] Ludmila Kazdová,[2] Ivan Mikšík,[1] Jan Neckář,[1] František Papoušek,[1] František Kolář,[1] Theodore W. Kurtz,[3] and Michal Pravenec[1]

[1]*Institute of Physiology Academy of Sciences of the Czech Republic, Prague, Czech Republic;* [2]*Institute for Clinical and Experimental Medicine, Prague, Czech Republic; and* [3]*Department of Laboratory Medicine, University of California, San Francisco, California*

Submitted 28 May 2014; accepted in final form 22 July 2014

Houštěk J, Vrbacký M, Hejzlarová K, Zídek V, Landa V, Šilhavý J, Šimáková M, Mlejnek P, Kazdová L, Mikšík I, Neckář J, Papoušek F, Kolář F, Kurtz TW, Pravenec M. Effects of mtDNA in SHR-mt^{F344} versus SHR conplastic strains on reduced OXPHOS enzyme levels, insulin resistance, cardiac hypertrophy, and systolic dysfunction. *Physiol Genomics* 46: 671–678, 2014. First published July 29, 2014; doi:10.1152/physiolgenomics.00069.2014.—Common inbred strains of the laboratory rat can be divided into four major mitochondrial DNA (mtDNA) haplotype groups represented by the BN, F344, LEW, and SHR strains. In the current study, we investigated the metabolic and hemodynamic effects of the SHR vs. F344 mtDNA by comparing the SHR vs. SHR-mt^{F344} conplastic strains that are genetically identical except for their mitochondrial genomes. Altogether 13 amino acid substitutions in protein coding genes, seven single nucleotide polymorphisms in tRNA genes, and 12 single nucleotide changes in rRNA genes were detected in F344 mtDNA compared with SHR mtDNA. Analysis of oxidative phosphorylation system (OXPHOS) in heart left ventricles (LV), muscle, and liver revealed reduced activity and content of several respiratory chain complexes in SHR-mt^{F344} conplastic rats compared with the SHR strain. Lower function of OXPHOS in LV of conplastic rats was associated with significantly increased relative ventricular mass and reduced fractional shortening that was independent of blood pressure. In addition, conplastic rats exhibited reduced sensitivity of skeletal muscles to insulin action and impaired glucose tolerance. These results provide evidence that inherited alterations in mitochondrial genome, in the absence of variation in the nuclear genome and other confounding factors, predispose to insulin resistance, cardiac hypertrophy and systolic dysfunction.

mitochondria; diabetes; heart mass; conplastic; spontaneously hypertensive rat

INBRED STRAINS OF THE LABORATORY rat carry four major haplotypes of mitochondrial DNA (mtDNA), which are represented by BN, F344, LEW, and SHR strains (8). To study the effects of mtDNA haplotypes on mitochondrial function as well as on metabolic and hemodynamic traits, we derived a series of conplastic strains by transferring the BN, LEW, and F344 mitochondrial genomes on the SHR genetic background by >10 backcrosses to SHR females. Since conplastic strains are genetically identical except for their mtDNA, any phenotypic differences can be potentially caused by naturally occurring variation in mtDNA. Our previous experiments showed that the SHR-mt^{BN} vs. SHR conplastic strains differ in multiple amino acid substitutions in mtDNA protein coding genes, including a unique mutation in *mt-Co1* in BN mtDNA that was associated with reduced mitochondrial cytochrome *c* oxidase activity and with major metabolic risk factors for Type 2 diabetes including impaired glucose tolerance, reduced skeletal muscle ATP and glycogen concentration, and insulin resistance (8). In addition, by the analysis of SHR-mt^{LEW} vs. SHR conplastic strains, we obtained evidence that inherited variation in mitochondrial *mt-Nd2, mt-Nd4*, and *mt-Nd5* genes encoding respiratory chain complex I subunits, in the absence of variation in the nuclear genome and other confounding factors, can influence glucose and lipid metabolism (3). In the current study, we report results obtained by analyses of the SHR-mt^{F344} vs. SHR conplastic strains. We found multiple differences in F344 vs. SHR mtDNA, including nonsynonymous substitutions in protein coding genes, as well as mutations in tRNA and rRNA genes that were associated with reduced cardiac oxidative phosphorylation system (OXPHOS) enzyme content and activities and cardiac hypertrophy with systolic dysfunction that was independent of blood pressure.

MATERIALS AND METHODS

Animals. We selectively replaced the mitochondrial genome of a highly inbred strain of spontaneously hypertensive rats (SHR) (SHR/OlaIpcv strain) with the mitochondrial genome of a highly inbred strain of F344 (F344/Crl) rats to create a novel SHR/OlaIpcv-mt^{F344} conplastic strain harboring the F344 mitochondrial genome on the SHR nuclear genetic background (SHR-mt^{F344}). We derived the conplastic strain using the "supersonic" breeding strategy of Behringer (1) to accelerate the breeding process (6). In the current experiments, we studied male conplastic rats after 10–12 generations of backcrossing. Genotype analysis of polymorphic markers distributed at ~10 cM intervals across the nuclear genome as previously described (8) confirmed lack of divergence in nuclear DNA between the SHR-mt^{F344} conplastic strain and the SHR progenitor strain. Thus, there is a very high probability that the conplastic and progenitor strains used in this study are homozygous and identical at any given locus in the nuclear genome. All experiments were performed in

Address for reprint requests and other correspondence: M. Pravenec, Inst. of Physiology Academy of Sciences of the Czech Republic v.v.i., Vídeňská 1083, 14220 Prague 4, Czech Republic (e-mail: pravenec@biomed.cas.cz).

Table 1. *Amino acid differences in mtDNA encoded OXPHOS protein subunits between F344 and SHR strains*

Gene	AA No.	Rat F344	Rat SHR	Human	Relevant Human mtDNA site	Nearby Human Pathology Mutation, AA No.	AA Character Hydrophobic/-philic R-chain	
							F344	SHR
mt-Nd2	150	Asn	Ser	Asn	hu 4918	LHON/IR/AMD/NRTI-PN 4917A>G, Asn150Asp	hydrophilic polar	hydrophilic polar
	265	Ala	Thr	Ala	hu 5262	LHON 5244G>A, Gly259Ser	tiny nonpolar	hydrophilic polar
	304	Thr	Met	Leu	hu 5380		hydrophilic polar	hydrophobic nonpolar
	318		His	Phe	hu 5419	progressive encephalomyopathy 5452C>T, Thr328Met		hydrophilic basic
mt-Nd4	23	Ile	Thr	Ile	hu 10827	MELAS 11084A>G, Thr109Ala	hydrophobic nonpolar	hydrophilic polar
	158	Ile	?	Leu	hu 11231	CPEO 11232T>C, Leu158Pro	hydrophobic nonpolar	
	356	Ala	Thr	Ala	hu 11825	exercise intolerance/oncocytoma 11832G>A, Trp359Ter	tiny nonpolar	hydrophilic polar
	393	Met	Ile	Leu	hu 11938	thyroid cancer cell line 11919C>T, Ser387Phe	hydrophobic nonpolar	hydrophobic nonpolar
	401	Val	Ile	Leu	hu 11960	OAT 11994C>T, Thr412Ile*	hydrophobic nonpolar	hydrophobic nonpolar
mt-Co1	406	Asp	Asn	Asp	hu 7119	prostate cancer 7083A>G, Ile394Val*	hydrophilic acidic	hydrophilic polar
mt-Co2	165	Ile	Val	Val	hu 8078	DEAF 8078G>A, Val165Ile	hydrophobic nonpolar	hydrophobic nonpolar
mt-Atp6	35	Glu	Lys	Lys	hu 8629	LHON 8668T>C, Trp48Arg	hydrophilic acidic	hydrophilic basic
mt-Cytb	214	Asp	Asn	His	hu 15386	possible LHON factor 15395A>G, Lys217Glu	hydrophilic acidic	hydrophilic polar

*Respective amino acid (AA) change in both F344 and SHR strains. AA No., position of amino acid in the respective subunit of F344 strain. ?, the amino acid could not be identified. AMD, age-related macular degeneration; CPEO, chronic progressive external ophthalmoplegia; DEAF, maternally inherited deafness; IR, insulin resistance; LHON, Leber hereditary optic neuropathy; MELAS, mitochondrial encephalomyopathy, lactic acidosis, and stroke-like episodes; NRTI-PN, antiretroviral therapy-associated peripheral neuropathy; OAT, oligoasthenoteratozoospermia.

agreement with the Animal Protection Law of the Czech Republic and were approved by the Ethics Committee of the Institute of Physiology, Academy of Sciences of the Czech Republic, Prague.

F344 mtDNA sequence analysis. We searched for variants by comparing the published F344 sequence (10) to the published mitochondrial genome sequences (accession # AC000022) of the BN (BN/SsNHsdMCW) and SHR/Ola strains.

Activities and protein content of mitochondrial oxidative phosphorylation enzymes and adenine nucleotide levels. Liver and heart ventricle homogenates (5%, wt/vol) were prepared in STE medium (0.25 M sucrose, 10 mM Tris·HCl, 1 mM EDTA, pH 7.4), 1 μg/ml protease inhibitor cocktail (PIC, Sigma P8340), and gastrocnemius muscle homogenates were prepared in KCl medium (150 mM KCl, 2 mM EDTA, 50 mM Tris·HCl, pH 7.4, 1 μg/ml PIC) with a motor-driven glass-Teflon homogenizer, filtered through 200 μm nylon mesh and frozen at −80°C.

We used spectrophotometric methods (9, 12) to measure enzyme activities of ferrocytochrome *c*:oxidoreductase [cytochrome *c* oxidase (COX), complex IV]; succinate:ferricytochrome *c* oxidoreductase, succinate cytochrome *c* reductase (SCCR), complexes II + III; rotenone sensitive NADH:ferricytochrome *c* oxidoreductase, NADH cytochrome *c* reductase (NCCR), complexes I + III; and citrate synthase (CS). Enzyme activity results are expressed per mg of homogenate protein.

We used SDS-PAGE and Western blotting of tissue homogenates to measure levels of a panel of mitochondrial respiratory chain proteins using specific antibodies and methods similar to those previously described (4). We have used primary mouse monoclonal antibodies (Abcam) to measure the levels of the 70 kDa subunit of succinate dehydrogenase (ab14715); α-subunit of the F_1F_o ATP synthase (ab14748); subunit 4 of cytochrome *c* oxidase (ab14744); core 2 subunit of ubiquinol:ferricytochrome *c* oxidoreductase (ab14745); and 39 kDa subunit of NADH:ubiquinone oxidoreductase (ab14713). We quantified the levels of these proteins by detection of infrared fluorescence with anti-mouse Alexa Fluor 680 or IRDye 800-labeled secondary antibodies and an Odyssey Infrared Imaging System (LI-COR Biotechnology, Lincoln, NE). Results are expressed as relative fluorescence units determined per mg of homogenate protein.

Liquid nitrogen snap-frozen samples of skeletal muscle, liver and heart were also processed in for measurement of the content of adenine nucleotides by high pressure liquid chromatography (2).

Tissue content of mtDNA. We used real-time PCR to measure DNA copy number of mitochondrial genes *mt-Co1, mt-Nd4, mt-Atp8*, and *mt-Cytb* relative to the amount of the nuclear gene cytochrome *c* oxidase, subunit IV, isoform 1 (*Cox4i1*) as an internal control. For real-time PCR, total DNA was isolated by standard methods and analyzed by real-time PCR testing using QuantiTect SYBR Green reagents (Qiagen, Valencia, CA) on an Opticon continuous fluores-

Table 2. *Sequence differences in tRNA mitochondrial genes between F344 and SHR strains*

tRNA	Nucleotide No.	Rat F344	Rat SHR	Change	Human	Relevant Human mtDNA Site	Nearby Human Pathology Mutation
Phe	32	TG–AA	TGAAA	ins A	TG–AA	hu 611	MERRF 611G>A
Cys	5196 (5198)	GGAGA	GGGGG	A>G	d.n.c.		
	5198 (5200)	AGATT	GGGTT	A>G	d.n.c.		
	5233 (5235)	GATAA	GAAAA	T>A	GAAAA	hu 5811	mitochondrial encephalopathy 5814T>C
Tyr	5265 (5267)	GGGCT	GGCCT	G>C	GGCCT	hu 5839	FSGS, mitochondrial cytopathy 5843A>G
Asp	6974 (6976)	AAGTT	AAATT	G>A	AAATT	hu 7559	myopathy, ataxia, nystagmus, migraines, LA 7554G>A
Thr	15329 (15331)	CAGTC	CAATC	G>A	CCTTT	hu 15941	MM 15940delT, possibly LVNC-associated 15942T>C

d.n.c., Does not correspond. Nucleotide No., the nucleic base position in mtDNA of F344 strain. The number in parenthesis is the nucleic base position in mtDNA of SHR strain, if it is different from F344 strain. FSGS, focal segmental glomerulosclerosis; MERRF, myoclonic epilepsy and ragged red muscle fibers; MM, mitochondrial myopathy; LA, lactic acidosis; LVNC, left ventricular noncompaction.

Table 3. *Sequence differences in rRNA mitochondrial genes between F344 and SHR strains*

rRNA	Nucleotide No.	Rat F344	Rat SHR	Change	Human	Relevant Human mtDNA Site	Nearby Human Pathology Mutation
12S	935	TGACA	TGGCA	A>G	– –AC–	hu 1507	DEAF 1494A>T
	942	CACAT	CATAT	C>T	CA–AA	hu 1512–	DEAF 1517A>C
16S	1132	AA–CC	AACCC	ins C	d.n.c.		
	1136 (1137)	CCACA	CCCCA	A>C	CCAGA	hu 1708	
	1222 (1223)	TGATG	TGGTG	A>G	AGATG	hu 1798	
	1247 (1248)	AACAA	AATAA	C>T	ATATA	hu 1823	
	1520 (1521)	TAGCC	TAACC	G>A	TAGTC	hu 2098	
	1584 (1585)	AATCA	AACCA	T>C	– –TAA	hu 2159	
	1653-4	TTACA	TT– –A	del AC	CTAAA	hu 2227-8	
	1717 (1716)	GATCC	GACCC	T>C	CACCC	hu 2282	possibly LVNC-associated 2352T>C
	1833 (1832)	TAGAA	TAAAA	G>A	CATTA	hu 2407	possibly LVNC-associated 2361G>A
	2171 (2170)	TTTAA	TTCAA	T>C	TTTAA	hu 2739	possibly LVNC-associated 2755A>G

cence detector (MJ Research, Waltham, MA) with an annealing temperature of 58°C. Mitochondrial DNA levels were normalized relative to the internal genomic DNA control with relative amounts mtDNA to genomic DNA determined in triplicate. The primers used to amplify mitochondrial genes were: *mt-Co1* upstream 5′- gga gca gta ttc gcc atc at, *mt-Co1* downstream 5′- cgg ccg taa gtg aga tga at; *mt-Cyb* upstream 5′- cat cag tca ccc aca tctg c, *mt-Cyb* downstream 5′- tgg atg gaa tgg gat ttt gt; *mt-Nd4* upstream 5′- ctc aca aca cac ccc cta cc, *mt-Nd4* downstream 5′- tcc cat aac ccc cta gct tt; *mt-Atp8* upstream 5′- tgc cac aac tag aca cat cca, *mt-Atp8* downstream 5′- tgt ggg ggt aat gaa aga gg. The primers used to amplify the nuclear gene *Cox4i1* were upstream 5′- act acc cct tgc ctg atg tg and downstream 5′- aca gat ctg cgc tca cac ac.

Metabolic phenotypes. After the rats were weaned, we fed the conplastic ($n = 10$) and control SHR rats ($n = 8$) standard chow and at 10 wk of age, switched them to a semisynthetic diet (Hope Farms) containing 60% fructose for 2 wk prior to study. In previous studies in the SHR, we have found that administration of a high-fructose diet can increase susceptibility to metabolic disturbances in this strain. At the end of the study, rats in the ad libitum fed state were euthanized with carbon dioxide, and then serum and tissues were collected for final biochemical analyses.

Oral glucose tolerance test. Oral glucose tolerance tests (OGTT) were performed after 2 wk of fructose feeding with a glucose load of 300 mg/100 g body wt after overnight fasting. Blood was drawn from the tail without anesthesia before the glucose load (0 min time point) and at 30, 60, and 120 min thereafter.

Biochemical analyses. Blood glucose levels were measured by the glucose oxidase assay (Erba-Lachema, Brno, Czech Republic) in tail vein blood drawn into 5% trichloroacetic acid and promptly centrifuged. Serum triglyceride concentrations were measured by standard enzymatic methods (Erba-Lachema, Brno, Czech Republic). Nonesterified fatty acids levels were determined with an acyl-CoA oxidase-based colorimetric kit (Roche Diagnostics, Mannheim, Germany). Serum insulin concentrations were determined with the Mercodia Rat Insulin ELISA kit (Mercodia, Uppsala, Sweden).

Muscle triglyceride measurements. For determination of triglycerides, gastrocnemius muscles were powdered under liquid N_2 and extracted for 16 h in chloroform-methanol, after which 2% KH_2PO_4 was added, and the solution was centrifuged. The organic phase was removed and evaporated under N_2. The resulting pellet was dissolved in isopropyl alcohol, and triglyceride content was determined by enzymatic assay (Erba-Lachema).

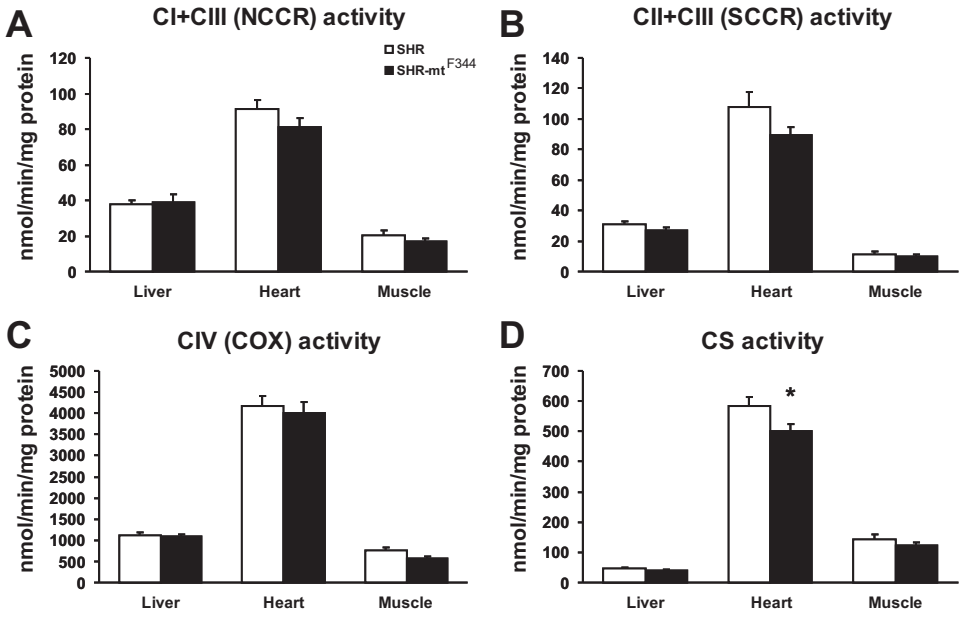

Fig. 1. Mitochondrial respiratory chain enzyme activities in tissue homogenates. Values are means ± SE from 9 rats in each group. *$P < 0.05$. See text for abbreviations.

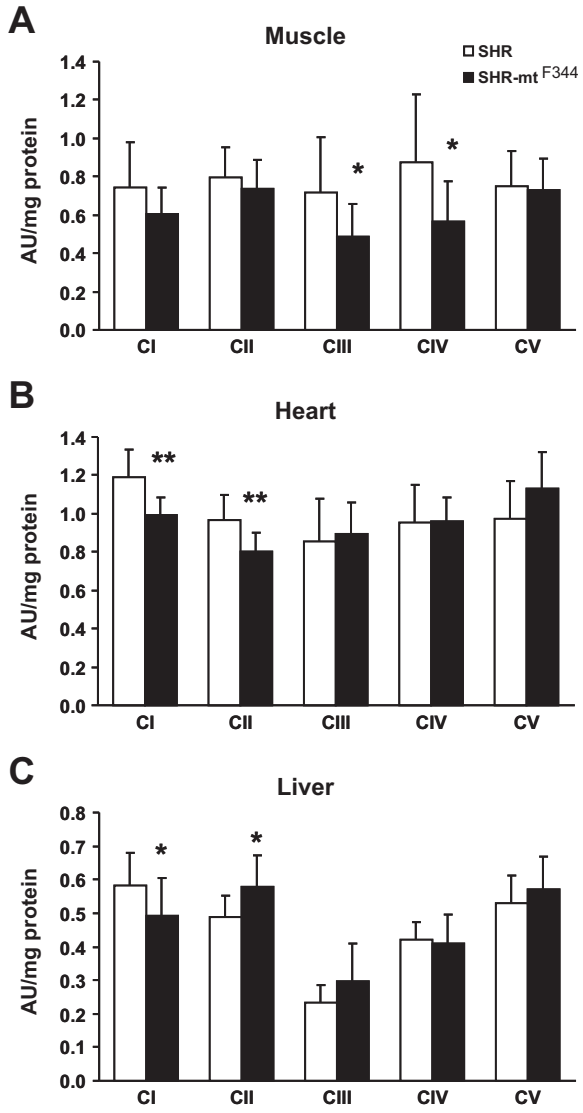

Fig. 2. Mitochondrial respiratory chain enzyme levels in tissue homogenates. Values are means ± SE from 9 rats in each group. *$P < 0.05$; **$P < 0.01$.

Glucose utilization in skeletal muscles. We determined glycogen synthesis in isolated diaphragm muscle by measuring the incorporation of ^{14}C-U glucose into glycogen. The muscles were attached to a stainless steel frame in situ at in vivo length by special clips and separated from other muscles and tendons and immediately incubated for 2 h in Krebs-Ringer bicarbonate buffer, pH 7.4, gaseous phase 95% O_2 and 5% CO_2 that contained 5.5 mM unlabeled glucose, 0.5 μCi/ml of ^{14}C-U glucose (UVVR, Prague, Czech Republic), and 3 mg/ml bovine serum albumin (Fraction V, Sigma) with or without 250 μU/ml insulin. After 2 h incubation, glycogen was extracted and glucose incorporation into glycogen determined.

Glucose utilization in isolated epididymal adipose tissue. Distal parts of epididymal adipose tissue were rapidly dissected and incubated for 2 h in Krebs-Ringer bicarbonate buffer with 5 mmol/l glucose, 0.1 μCi ^{14}C-U-glucose/ml, and 2% bovine serum albumin, gaseous phase 95% O_2 and 5% CO_2 in the presence (250 μU/ml) or absence of insulin in incubation media. All incubations were performed at 37°C in sealed vials in a shaking water bath. Estimation of ^{14}C-glucose incorporation into neutral lipids was performed. Adipose tissue was removed from incubation medium, rinsed in saline, and immediately put into chloroform. The pieces of tissue were dissolved with a Teflon pestle homogenizer, methanol was added (chloroform-methanol 2:1), and lipids were extracted at 4°C overnight. The remaining tissue was removed, KH_2PO_4 was added, and a clear extract was taken for further analysis. An aliquot was evaporated and reconstituted in scintillation liquid, and the radioactivity measured by scintillation counting. Incremental glucose utilization was calculated as the difference between the insulin stimulated and basal incorporation of glucose into neutral lipids.

Blood pressure measurements. Arterial blood pressure was measured continuously by radiotelemetry in paired experiments between conscious, unrestrained male conplastic rats ($n = 8$) and SHR controls ($n = 8$) fed a standard diet starting at the age of 10 wk. All rats were allowed to recover for at least 7 days after surgical implantation of radiotelemetry transducers before the start of blood pressure recordings. Pulsatile pressures were recorded in 5 s bursts every 10 min throughout the day and night, and 24 h averages for systolic arterial blood pressure were calculated for each rat for 1 wk periods. After measuring blood pressure for 2 wk, we gave all rats 1% NaCl for drinking instead of tap water for an additional week of blood pressure measurements to test for effects of the F344 vs. SHR mtDNA on blood pressure salt sensitivity. The results from each rat in the same group were then averaged to obtain the group means.

Echocardiography. Transthoracic echocardiography was performed using the GE Vivid 7 Dimension (GE Vingmed Ultrasound, Horten, Norway) with a 12 MHz linear matrix probe M12-L in 3 mo old animals fed a standard diet. Left ventricular two-dimensional images were obtained in the parasternal long- and short-axis views, and M-mode images were acquired in the long-axis view under isoflurane (2%) inhalation anesthesia (Aerrane, Baxter, SA). The measurements included heart rate (HR), end-diastolic diameter (LVD_d), end-systolic diameter (LVD_s), diastolic and systolic anterior wall thickness, and diastolic and systolic posterior wall thickness. The main functional parameter, percent fractional shortening (FS) was calculated as follows: $FS = 100*(LVD_d - LVD_s)/LVD_d$. At least three measurements were performed in every mode/view and averaged for each rat. After the assessment of the baseline parameters, the maximum response to dobutamine infused into the jugular vein (15 and 30 mg/kg, 4 min each) was obtained. The person evaluating the images was blinded for the experimental group.

Statistical analysis. We used Student's *t*-test to analyze for differences between group means with statistical significance defined as $P < 0.05$. All results are expressed as means ± SE.

Table 4. *Adenine nucleotide levels*

Trait	SHR	SHR-mt^{F344}
	Gastrocnemius muscle	
ATP	1387.67 ± 46.37	1405.44 ± 18.94
ADP	387.78 ± 15.57	390.89 ± 10.01
AMP	23.11 ± 3.00	22.89 ± 3.03
ATP/ADP	3.61 ± 0.14	3.61 ± 0.08
Energy charge	0.88 ± 0.00	0.88 ± 0.00
	Heart	
ATP	654.22 ± 34.64	661.56 ± 16.62
ADP	560.67 ± 24.38	591.00 ± 19.77
AMP	299.22 ± 22.20	330.00 ± 27.13
ATP/ADP	1.17 ± 0.03	1.13 ± 0.04
Energy charge	0.62 ± 0.01	0.61 ± 0.01
	Liver	
ATP	449.11 ± 30.12	496.33 ± 47.45
ADP	483.00 ± 21.90	518.67 ± 39.82
AMP	369.89 ± 14.64	402.33 ± 36.67
ATP/ADP	0.92 ± 0.03	0.96 ± 0.05
Energy charge	0.53 ± 0.01	0.53 ± 0.02

Values are means ± SE from 9 rats. Levels of AMP, ADP, and ATP are expressed in nmol/g per 100 mg wet wt.

Table 5. *Parameters of lipid and glucose metabolism*

Trait	SHR	SHR-mt^{F344}
Serum glucose, mmol/l	6.6 ± 0.2	6.3 ± 0.2
Serum insulin, mmol/l	0.4 ± 0.03	0.53 ± 0.08
Serum triglycerides, mmol/l	2.32 ± 0.18	1.76 ± 0.10*
Serum NEFA, mmol/l	0.35 ± 0.04	0.28 ± 0.02
Heart triglycerides, μmol/g	1.2 ± 0.1	1.3 ± 0.2
Liver triglycerides, μmol/g	8.2 ± 0.9	9.4 ± 1.1
Gastrocnemius muscle triglycerides, μmol/g	11.3 ± 1.2	9.9 ± 1.1

Values are means ± SE from 10 conplastic and 8 control rats, *$P < 0.05$. NEFA, nonesterified fatty acids.

RESULTS

F344 mitochondrial DNA sequence analysis. Comparison of the published F344 mtDNA sequence (10) with the SHR mtDNA revealed 13 amino acid substitutions in mtDNA protein coding genes (four in *mt-Nd2*, five in *mt-Nd4*, one in *mt-Co1*, one in *mt-Co2*, one in *mt-Atp6*, and one in *mt-Cytb*). Seven differences in protein-coding genes were located close to mutations associated with known human pathologies: two of them are in *mt-Nd2* gene [Leber hereditary optic neuropathy (LHON), insulin resistance], three in *mt-Nd4* gene (chronic progressive external ophthalmoplegia, exercise intolerance, and cancer), one in *mt-Co2* gene (maternally inherited deafness), and one in *mt-Cytb* gene (LHON) (Table 1). Interestingly, three amino acid substitutions occurred exactly at positions of human pathological mutation (*mt-Nd2* Ser150Asn, *mt-Nd4* ?158Ile, *mt-Co2* Val165Ile). Of these the *mt-Co2* Val165Ile substitution was identical with human mtDNA mutation associated with maternally inherited deafness and affected the amino acid highly conserved in higher eukaryotes. However, the substitution had only minor effect on the character of this amino acid.

There were also seven nucleotide substitutions affecting five tRNA genes. Compared with human mtDNA, five of these variations were located very close to described positions of human pathogenic mutations. As is shown in Table 2, these pathologies include severe diseases like myoclonic epilepsy and ragged red muscle fibers, mitochondrial encephalopathy, cytopathy and myopathy, focal segmental glomerulosclerosis, lactic acidosis, and left ventricular noncompaction (LVNC). The rRNA mtDNA genes displayed also numerous differences between F344 and SHR strains. In the 12S rRNA gene there are only two one-nucleotide changes, but there are multiple sequence differences in the gene for 16S rRNA (Table 3). Since human and rat 12S and 16S rRNA sequences differ quite a lot, there are only few human pathologies associated with mutations in the rRNA's genes close to the relevant rat sequence where SHR and F344 strain are different. In general, these close mutations in 12S rRNA are in human mostly associated with maternally inherited deafness. In contrast, mutations in 16S rRNA are in humans mostly

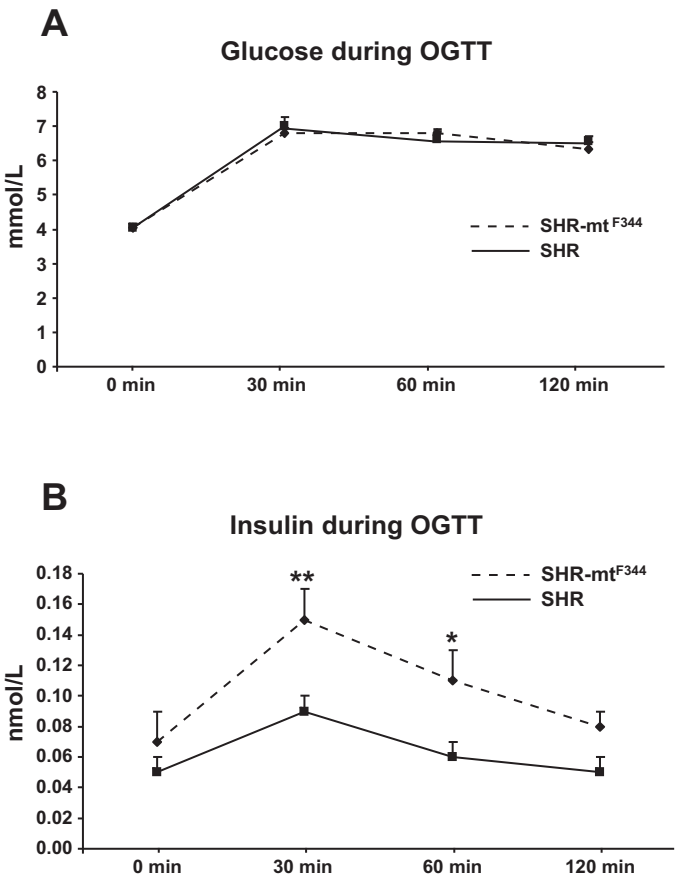

Fig. 3. Oral glucose tolerance test (OGTT). *A*: blood glucose levels before and after glucose administration in the SHR progenitor strain (solid line) and the SHR-mt^{F344} conplastic strain (dashed line). After oral glucose loading, the SHR conplastic strain showed similar glucose levels compared with the SHR progenitor strain. *B*: serum insulin levels before and after oral glucose administration. Same symbols as for serum glucose results. After oral glucose loading, the SHR-mt^{F344} conplastic strain showed significantly greater area under the curve for serum insulin levels than the SHR progenitor strain ($P < 0.01$). Values are means ± SE from 10 conplastic and 8 control rats. *$P < 0.05$; **$P < 0.01$.

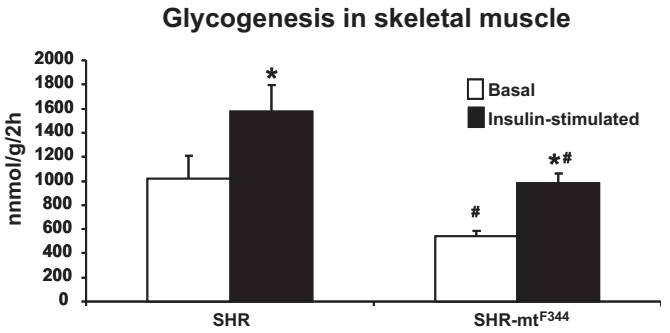

Fig. 4. Basal and insulin stimulated glycogenesis. SHR-mt^{F344} conplastic rats showed significantly lower both basal (open bars) and insulin-stimulated (solid bars) incorporation of radioactively labeled glucose into skeletal muscle glycogen compared with SHR progenitor rats. Values are means ± SE from 10 conplastic and 8 control rats. *$P < 0.05$; #$P < 0.01$.

Table 6. *Parameters of heart physiology*

Parameter	SHR	SHR-mt^{F344}
BW, g	387 ± 7	382 ± 9
RVW, mg	203 ± 7	219 ± 8
LVW, mg	1031 ± 22	1071 ± 20
RVW/BW, mg/g	0.531 ± 0.016	0.572 ± 0.009*
LVW/BW, mg/g	2.695 ± 0.022	2.807 ± 0.034*

Values are means ± SE from 6 rats in each group; *$P < 0.05$ (unpaired *t*-test). BW, body weight; RVW, right ventricular weight; LVW, left ventricular weight including the interventricular septum.

Table 7. *Echocardiography assessment of left ventricular function in SHR vs. SHR-mt^{F344} conplastic rats*

Parameter	SHR	SHR-mt^{F344}
HR, beats/min	324 ± 7	331 ± 8
LVD_d, mm	7.98 ± 0.07	8.35 ± 0.29
LVD_s, mm	5.02 ± 0.08	5.60 ± 0.22*
AWT_d, mm	1.93 ± 0.05	1.91 ± 0.10
PWT_d, mm	2.03 ± 0.10	1.85 ± 0.09
AWT_s, mm	3.12 ± 0.13	3.03 ± 0.12
PWT_s, mm	3.02 ± 0.11	2.70 ± 0.10
FS, %	37.1 ± 1.0	33.4 ± 0.9*
FS_{max}, %	89.6 ± 0.2	86.1 ± 0.9†

Values are means ± SE from 6 rats in each group; *$P < 0.05$; †$P < 0.01$. HR, heart rate; LVD_d, end-diastolic diameter; LVD_s, end-systolic diameter; AWT_d and AWT_s, anterior wall thickness in diastole and systole, respectively; PWT_d and PWT_s, posterior wall thickness in diastole and systole, respectively; FS, fractional shortening at baseline; FS_{max}, maximum FS after dobutamine infusion.

associated with LVNC, then with Rett syndrome, myopathy, MELAS, and with Alzheimer's and Parkinson's diseases (http://www.mitomap.org); the closest three mutations are shown in Table 3.

Mitochondrial OXPHOS enzyme activities. Analysis of mitochondrial OXPHOS system in tissue homogenates revealed a general tendency of a decrease in OXPHOS enzyme-specific activities NCCR, SCCR, COX, and CS in SHR-mt^{F344} conplastic rats vs. SHR strain (Fig. 1). The decrease was more pronounced in heart and muscle than in liver.

Mitochondrial OXPHOS enzyme content and mtDNA copy number. Western blot analysis using monoclonal antibodies to selected marker subunits of individual enzyme complexes of mitochondrial respiratory chain further revealed a decrease in several complexes in SHR-mt^{F344} conplastic rats compared with SHR strain. Based on their specific content per mg protein of tissue homogenate, complexes III and IV were significantly decreased in muscle and complexes I and II in heart, while in liver complex I was decreased and complex II was increased (Fig. 2). There were no significant differences in mtDNA copy number (data not shown).

Adenine nucleotide levels. HPLC analysis of tissue content of adenine nucleotides ATP, ADP, and AMP revealed similar relative contribution of ATP and ADP and smaller of AMP to the total nucleotide levels in heart and liver, while in muscle the ATP was most abundant and AMP was very low. Comparison of SHR-mt^{F344} conplastic rats with SHR strain indicated a small insignificant decrease in ATP/ADP ratio in heart of SHR-mt^{F344} but not in liver or muscle (Table 4).

Metabolic phenotypes in SHR-mt^{F344} conplastic rats. The mean body weight of the conplastic strain was similar to the SHR strain (329 ± 5 vs. 325 ± 4 g). Serum glucose levels were similar between the SHR-mt^{F344} conplastic and the SHR progenitor strain, while the insulin concentrations tended to be higher in conplastic rats (Table 5). During OGTT, conplastic rats showed glucose levels similar to SHR controls. On the other hand, insulin levels were significantly increased in conplastic rats after glucose loading (Fig. 3), which suggests insulin resistance. Conplastic rats showed significantly reduced nonfasting serum triglyceride levels, while triglyceride levels in liver, skeletal muscle, and heart were similar in conplastic and SHR controls (Table 5).

Figure 4 shows basal and insulin-stimulated incorporation of radioactively labeled glucose into skeletal muscle glycogen. In the SHR-mt^{F344} conplastic strain, glucose incorporation into skeletal muscle glycogen was significantly lower than in the SHR progenitor strain both before and after stimulation with insulin. The insulin-induced increase in nonoxidative glucose metabolism was significantly lower in the conplastic rats than in the SHR controls (442 ± 58 vs. 704 ± 129 $nmol \cdot g^{-1} \cdot 2\ h^{-1}$, $P < 0.05$). There were no significant differences in basal or insulin-stimulated incorporation of glucose into adipose tissue lipids between conplastic and control rats (data not shown).

Blood pressures, heart mass, and function. There was no significant difference between SHR-mt^{F344} conplastic strain and SHR controls in systolic and diastolic blood pressures and HRs (data not shown). The weights of both heart ventricles normalized to body weight were significantly increased in SHR-mt^{F344} conplastic rats compared with SHR control (Table 6). There were no echocardiographically detectable differences in LV dimension and wall thickness between the two groups, except for the increased end-systolic diameter in conplastic rats. In addition, conplastic rats exhibited slight but significant impairment of FS both at baseline and after stimulation with dobutamine compared with the SHR (Table 7).

DISCUSSION

Recently, we demonstrated in SHR vs. SHR-mt^{BN} and in SHR vs. SHR-mt^{LEW} conplastic rats that naturally occurring variation in mtDNA in the absence of nuclear genome variation

Table 8. *Summary of phenotypic effects associated with transfer of major mtDNA haplotypes on SHR genetic background*

Traits	SHR vs. Conplastic Strains		
	SHR-mt^{BN}	SHR-mt^{LEW}	SHR-mt^{F344}
Body weight	↓	↑	↔
Serum triglycerides	↔	↔	↓
Glucose during OGTT	↑	↔	↔
Insulin during OGTT	↑	n.d.	↑
Muscle glycogenesis	↓	↓	↓
Left ventricular mass	n.d.	n.d.	↑
Fractional shortening	n.d.	n.d.	↓
RCH complexes CI, CII, CIII, CIV, CV activity and/or content	CIV ↓	CI ↓, CII ↓, CIII ↓, CIV ↓, CV ↓	CI ↓, CII ↓, CIII ↓, CIV ↓
Tissue specificity of RCH complexes decrease	liver	muscle>>heart>liver	heart>>muscle>liver

↑, ↓, and ↔ symbols denote significantly increased, decreased, and not significantly different, respectively, values in conplastic strains when compared with the SHR. n.d., Not determined; RCH, respiratory chain; CI–CV, complexes I–V.

is associated with selective reduction in content and activity of OXPHOS enzymatic complexes in skeletal muscle and several risk factors for Type 2 diabetes but with no significant differences in blood pressure or cardiac mass (3, 8). In the present studies, we analyzed phenotypic effects of the mtDNA haplotype of the F344 strain, which is only distantly related to the SHR. Similar to SHR-mt^{BN} and SHR-mt^{LEW} conplastic strains, the SHR-mt^{F344} conplastic rats exhibited reduced content and activity of OXPHOS protein complexes compared with SHR controls and similar reduction of muscle glycogenesis and increased insulin levels during OGTT (for comparison see Table 8). In addition, replacement of mtDNA further caused a mild increase in heart mass in the SHR-mt^{F344} rats, which was independent of blood pressure because conplastic rats were hypertensive, similar to the SHR. Moreover, SHR-mt^{F344} conplastic rats exhibited small but significant impairment of cardiac systolic function both at baseline and after the stimulation with dobutamine. These results suggest that the original mtDNA haplotype of the SHR provides a relative protection against LV hypertrophy induced by spontaneous hypertension as well as against resistance of skeletal muscles to insulin action and glucose intolerance, while the mtDNA of F344 origin is less protective. The responsible mechanisms might be linked to reduced content and enzymatic activities of OXPHOS enzymes, as they are the only cellular components containing mtDNA-encoded proteins. Sequence differences between SHR and F344 mtDNA are numerous and include both the protein coding and tRNA genes and may thus affect several components of the OXPHOS system, in accordance with observed changes in the content of different OXPHOS complexes. Several differences in SHR/F344 mtDNA genes encoding OXPHOS subunits affected amino acids whose mutations were found to be pathological in humans (http://www.mitomap.org), and several other changes were closely apposed to established human pathological mutations. The conplastic model of SHR convincingly indicates that phenotypical changes at organ and organism levels are direct consequences of the changes in mtDNA-OXPHOS, but the further biochemical links remain to be elucidated. ATP production and mitochondrially generated reactive oxygen species (ROS) represent primary metabolites produced by OXPHOS system. We were unable to find significant differences in adenine nucleotide levels by HPLC analysis, which reflects the total cellular nucleotides but does not allow for detection of in situ changes in different subcellular compartment.

Recently, Kumarasamy et al. (5) reported analyses of reciprocal conplastic strains derived from SHR and SS (salt sensitive) strains. While no significant differences were observed in the SHR-mt^{SS} conplastic strain with mtDNA of the SS/Jr (salt sensitive) origin in heart weight, blood pressure, treadmill aerobic capacity, ROS production, or mtDNA copy number compared with SHR progenitor strain, the reciprocal SS-mt^{SHR} conplastic strain with mtDNA of SHR origin on the SS genetic background exhibited significantly increased aerobic capacity and survival time compared with SS progenitor strain. These results suggest that SHR mtDNA is protective compared with the SS mtDNA, which is consistent with our findings in SHR conplastic strains in which mtDNA of BN, LEW, and F344 origin was associated with reduced activities of OXPHOS complexes and metabolic disturbances compared with SHR progenitor strain.

In addition, Sethumadhavan et al. (11) reported that the T2DN-mt^{FHH} conplastic strain, which carries mtDNA of Fawn Hooded Hypertensive origin on a genetic background of the T2DN/Mcwi strain, a model of diabetic nephropathy closely related to Goto-Kakizaki strain (7), exhibited significantly decreased complex I and complex IV activities, reduced ATP levels in heart tissue, and increased left ventricular diastolic and systolic dimensions but no significant differences in left ventricular mass or left ventricular systolic function compared with the T2DN-mt^{Wistar} strain (11). However, these findings are difficult to compare to results of the current study because of differences between mtDNA haplotypes and genetic backgrounds of SHR vs. T2DN strains, when complex interactions between nuclear and mitochondrial genomes can affect mitochondrial function and cardiometabolic traits.

In summary, we have found that inherited variation in mitochondrial genes encoding respiratory chain complexes can influence mitochondrial function, glucose tolerance, and sensitivity of skeletal muscle to insulin action as well as cardiac remodeling and function. These results should serve to motivate future studies of the role of naturally occurring variation of mtDNA in the pathogenesis of cardiometabolic traits in humans.

GRANTS

This work was supported by the Ministry of Education, Youth and Sports of the Czech Republic (ERC CZ program grant LL1204 and RVO:67985823), by the Grant Agency of the Czech Republic (grants 14-36804G and 13-10267S), by the European Union EURATRANS award (HEALTH-F4-2010-241504), and by grant MH CZ - DRO ("Institute for Clinical and Experimental Medicine - IKEM, IN 0002301").

DISCLOSURES

No conflicts of interest, financial or otherwise, are declared by the author(s).

AUTHOR CONTRIBUTIONS

Author contributions: J.H., T.W.K., and M.P. conception and design of research; J.H., M.V., K.H., V.L., J.S., M.S., P.M., L.K., I.M., J.N., F.P., F.K., T.W.K., and M.P. analyzed data; J.H. and M.P. interpreted results of experiments; J.H., F.K., T.W.K., and M.P. drafted manuscript; J.H., V.Z., V.L., J.S., M.S., P.M., L.K., I.M., J.N., F.P., F.K., T.W.K., and M.P. approved final version of manuscript; M.V., K.H., V.Z., V.L., J.S., M.S., P.M., L.K., I.M., J.N., and F.P. performed experiments; M.P. prepared figures.

REFERENCES

1. **Behringer R.** Supersonic congenics? *Nat Genet* 18: 108, 1998.
2. **Flachs P, Novotný J, Baumruk F, Bardová K, Bouřová L, Mikšík I, Šponarová J, Svoboda P, Kopecký J.** Impaired noradrenaline-induced lipolysis in white fat of aP2-Ucp1 transgenic mice is associated with changes in G-protein levels. *Biochem J* 364: 369–376, 2002.
3. **Houštek J, Hejzlarová K, Vrbacký M, Drahota Z, Landa V, Zídek V, Mlejnek P, Šimáková M, Šilhavy J, Mikšík I, Kazdová L, Oliyarnyk O, Kurtz T, Pravenec M.** Nonsynonymous variants in mt-Nd2, mt-Nd4, and mt-Nd5 are linked to effects on oxidative phosphorylation and insulin sensitivity in rat conplastic strains. *Physiol Genomics* 44: 487–494, 2012.
4. **Ješina P, Tesařová M, Fornůsková D, Vojtíšková A, Pecina P, Kaplanová V, Hansiková H, Zeman J, Houštěk J.** Diminished synthesis of subunit a (ATP6) and altered function of ATP synthase and cytochrome c oxidase due to the mtDNA 2 bp microdeletion of TA at positions 9205 and 9206. *Biochem J* 383: 561–571, 2004.
5. **Kumarasamy S, Gopalakrishnan K, Abdul-Majeed S, Partow-Navid R, Farms P, Joe B.** Construction of two novel reciprocal conplastic rat strains and characterization of cardiac mitochondria. *Am J Physiol Heart Circ Physiol* 304: H22–H32, 2013.
6. **Landa V, Zídek V, Pravenec M.** Generation of rat "supersonic" congenic/conplastic strains using superovulation and embryo transfer. *Methods Mol Biol* 597: 267–275, 2010.
7. **Nobrega MA, Fleming S, Roman RJ, Shiozawa M, Schlick N, Lazar J, Jacob HJ.** Initial characterization of a rat model of diabetic nephropathy. *Diabetes* 53: 735–742, 2004.

8. **Pravenec M, Hyakukoku M, Houštěk J, Zídek V, Landa V, Mlejnek P, Mikšík I, Dudová-Mothejzíková K, Pecina P, Vrbacký M, Drahota Z, Vojtíšková A, Mráček T, Kazdová L, Oliyarnyk O, Wang J, Ho C, Qi N, Sugimoto K, Kurtz T.** Direct linkage of mitochondrial genome variation to risk factors for type 2 diabetes in conplastic strains. *Genome Res* 17: 1319–1326, 2007.
9. **Rustin P, Chretien D, Bourgeron T, Gerard B, Rotig A, Saudubray JM, Munnich A.** Biochemical and molecular investigations in respiratory chain deficiencies. *Clin Chim Acta* 228: 35–51, 1994.
10. **Schlick NE, Jensen-Seaman MI, Orlebeke K, Kwitek AE, Jacob HJ, Lazar J.** Sequence analysis of the complete mitochondrial DNA in 10 commonly used inbred rat strains. *Am J Physiol Cell Physiol* 291: C1183–C1192, 2006.
11. **Sethumadhavan S, Vasquez-Vivar J, Migrino RQ, Harmann L, Jacob HJ, Lazar J.** Mitochondrial DNA variant for complex I reveals a role in diabetic cardiac remodeling. *J Biol Chem* 287: 22174–22182, 2012.
12. **Wharton DC, Tzagoloff A.** Cytochrome oxidase from beef heart mitochondria. *Meth Enzymol* 10: 245–253, 1967.